

# Off-on Fluorescent Sensor from On-off Sensor: Exploiting Silver Nanoparticles Influence on the Organic Fluorophore Fluorescence

P. S. Hariharan · Arvind Sivasubramanian ·  
Savarimuthu Philip Anthony

Received: 25 September 2013 / Accepted: 20 November 2013 / Published online: 28 November 2013  
© Springer Science+Business Media New York 2013

**Abstract** Turn-off fluorescence of organic fluorophore, 2- {[4-(2H-Naphtho[1,2-d][1,2,3]triazol-2-yl)-phenyl]carboxylic acid (NTPC), with metal ions ( $\text{Fe}^{3+}$ ,  $\text{Cu}^{2+}$ ,  $\text{Pb}^{2+}$ ) was converted into turn-on fluorescent sensor for biologically important  $\text{Zn}^{2+}$ ,  $\text{Cu}^{2+}$  and  $\text{Fe}^{3+}$  metal ions in aqueous solution at ppb level by exploiting strong fluorescence quenching phenomena of metal nanoparticles when organic fluorophores assembled in the vicinity of metallic surface. Amino acid attached phenolic ligands (L) were used as reducing as well as functional capping agents in the synthesis of silver nanoparticles (AgNPs). The hydrogen bonding functionality of L facilitated the assembling of NTPC in the vicinity of metallic surfaces that leads to complete quenching of NTPC fluorescence. The strong and selective coordination of L with metal ions ( $\text{Zn}^{2+}$ ,  $\text{Cu}^{2+}$  and  $\text{Fe}^{3+}$ ) separates the NTPC from the AgNPs surface that turn-on the NTPC fluorescence. HR-TEM and absorption studies confirm the metal coordination with L and separation of NTPC from the AgNPs surface.  $\text{Mn}^{2+}$  showed selective red shifting of NTPC fluorescence after 12 h with all sample. Effects of different amino acid attached phenolic ligands were explored in the metal ion sensitivity and selectivity. This approach demonstrates the multifunctional utility of metal NPs in the development of turn-on fluorescence sensor for paramagnetic heavy metal ions in aqueous solution.

**Keywords** Heavy metal ions sensor · Turn-on fluorescent sensor fabrication · Nanoparticles-organic fluorophore hybrid sensor · Supramolecular chemistry

## Introduction

Exploration on chemosensors that can exhibit highly selective and sensitive binding affinity towards transition metal ions has attracted wide interest due to their crucial roles in various biological and environmental processes [1–5].  $\text{Cu}^{2+}$  and  $\text{Zn}^{2+}$  ions are indispensable trace elements existing as catalytic cofactors for a variety of metallo-enzymes and proteins and plays important role in various physiological and pathological processes [6, 7]. Under normal physiological conditions, brain requires higher level of  $\text{Cu}^{2+}$  compared to other parts of the body, but its excess accumulation causes neurodegenerative ailments like Alzheimer's, Wilson's, and Menke's diseases [8]. Zinc-binding proteins such as metallothionein carry out detoxification of lead by sequestering lead within enterocytes [7]. Iron is a ubiquitous metal in cells, it being present in the structure of many enzymes and proteins and therefore essential for cellular metabolism and enzyme catalysis [9]. Consequently, deficiency in  $\text{Fe}^{3+}$  leads to anemia, liver and kidney damages, diabetes, and heart diseases [10, 11]. These beneficial as well as detrimental roles of transition metal ions have prompted researchers to develop efficient methods for selective and sensitive assay of the metal ions both in vitro and in vivo [12, 13]. Of the different kinds of sensing, fluorescence based approach has many advantages due to its high sensitivity, straightforward application and real-time

P. S. Hariharan · A. Sivasubramanian · S. P. Anthony (✉)  
School of chemical & Biotechnology, SASTRA University,  
Thanjavur 613 403, Tamil Nadu, India  
e-mail: philip@biotech.sastra.edu

monitoring with fast response time [1–5, 14–17]. Particularly, developing a turn-on fluorescence sensor for heavy metal ions received significant attention because of its ease of detection [18, 19]. However, the paramagnetic nature of the transition elements such as  $\text{Cu}^{2+}$  and  $\text{Fe}^{3+}$  often leads to selective turn-off fluorescence and very rarely showed turn-on fluorescence.

The recent emergence of nanoscience and nanotechnology offered interesting opportunities to fabricate materials with enhanced/desired properties for various applications across physics, chemistry, biology and other interdisciplinary area of science and technology. For instance, the strong, unique and distance dependent optical properties of silver (Ag) and gold (Au) metal nanoparticles (NPs) that can be chemically engineered via surface functionalization have been successfully employed to develop colorimetric sensor for biological molecules as well as heavy metal ions [20–27]. Ag and AuNPs surfaces also exert a strong influence on the fluorescence properties of fluorophores placed in their vicinity. Two opposite phenomena was observed depending on the separation distance between NPs surface and fluorophores. Strong quenching of fluorescence intensity with a dramatic reduction on the excited states lifetimes were reported when the separation distance is smaller than 5 nm [28–31]. Whereas in the separation distance range of 10–20 nm, enhanced fluorescence emission was observed because of local concentration of the incident excitation field by the metallic nanoparticles [32–34]. The metal enhanced fluorescence has been widely exploited in the molecular fluorescence measurements and biosensors to increase the sensitivity and adaptability [35–37]. The strong fluorescence quenching properties of metal NPs could be employed to develop turn-on fluorescence sensor for heavy metal ions by choosing right capping ligands. The capping ligands should have both NPs stabilization and selective metal ions interacting functionality. The selective binding of metal ions with surface functionality of NPs is expected to separate the fluorophore from NPs surface vicinity that would re-generate the fluorescence.

Chemical molecules with 1, 2, 3-triazole unit in the structure have been utilized as intermediates for the synthesis of several products such as dyes [38] or optical brighteners [39]. Interestingly, naphthotriazoles exhibit intense fluorescence in the near UV and visible regions with high fluorescence quantum yield (>50 %, [40]) which is comparable to that of highly fluorescent compounds such as 1-aminonaphthalene or 9,10-diphenylanthracene [41]. Hence, naphthotriazoles are used as whitening agents [42], fluorescent probes with peptides [41] and sulfonated derivatives of 2H-naphthotriazoles are well-known in the textile industry [43]. Naphthotriazoles with different chemical functionalities including carboxylic and sulfonic acid that makes it water soluble showed strong fluorescence both in organic and aqueous solution.

The easy ionization properties of phenolic groups have been made use in the synthesis of AgNPs in the past [44].

Organic ligands based on amino acid attached phenols exhibited versatile coordination with different metal ions that resulted in the formation of intriguing structures including helical supramolecular structures in the solid state [45–47]. Hence, amino acid attached phenolic ligands could be directly used in the synthesis and stabilization of AgNPs that might also provide metal ions interacting surface functionality. Further such organic functionality could be used to assemble organic fluorophore via supramolecular interactions near the vicinity of metal NPs surface. In the present work, we report the strong fluorescence quenching of NTPC in aqueous solution by assembling in the vicinity of AgNPs surface and complete turn-on fluorescence upon addition of biologically important metal ions such as  $\text{Zn}^{2+}$ ,  $\text{Cu}^{2+}$  and  $\text{Fe}^{3+}$  (Scheme 1). The hydrogen bonding functionalities of phenolic amino acid ligands (L) of AgNPs and NTPC plays important role to facilitate the fluorophore assembling in the vicinity of NPs surfaces. The strong and selective coordination of L with metal ions ( $\text{Zn}^{2+}$ ,  $\text{Cu}^{2+}$  and  $\text{Fe}^{3+}$ ) separates the NTPC from the AgNPs surface that leads to complete regeneration of fluorescence. HR-TEM and absorption studies confirm the metal ions interaction with L-AgNPs. Effect of amino acid modification on the metal ions sensitivity and selectivity was also explored. The present approach demonstrates the multifunctional utility of metal NPs and an easy development of turn-on fluorescence sensor for paramagnetic heavy metal ions in aqueous solution.

## Experimental Section

**Chemicals** Amino acid, ethanol, p-aminobenzoic acid,  $\text{Cu}(\text{OAc})_2$ , pyridine, HCl,  $\text{NaNO}_2$ , DMF, DMSO and NaOH were obtained from Ranbaxy, India and used as received. Salicylaldehyde, 2-aminonaphthalene,  $\text{NaBH}_4$ ,  $\text{AgNO}_3$ , poly(vinyl alcohol) (PVA, M.Wt) were obtained from Sigma-Aldrich and were used as received. All the heavy metal salt solutions used for the experiments were prepared by mixing the requisite amount of salt in Mill-Q water. NTPC was synthesized following the literature procedure [48]. Amino acid attached phenolic chelating ligands were synthesized according to the reported procedure [45–47].

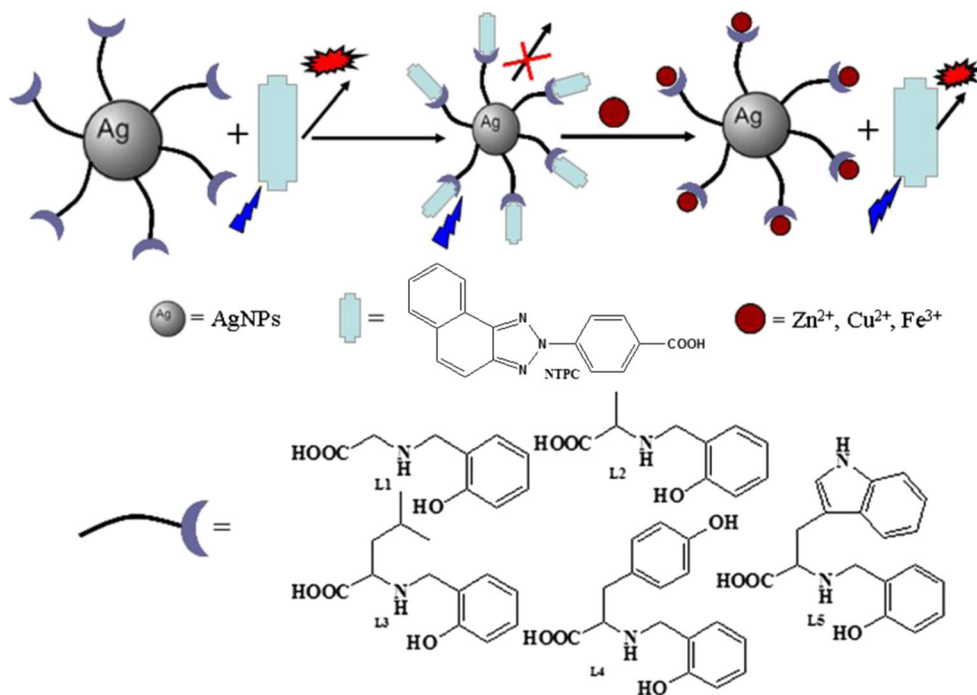
### General Procedures for the Synthesis

of 2-[4-(2H-Naphtho[1,2-d][1,2,3]triazol-2-yl)-phenyl] carboxylic acid (NTPC)

### Diazotization

To a solution of p-aminobenzoic acid (6 mmol) in  $\text{H}_2\text{O}$  (13.0 mL), concentrated HCl (2.8 mL; 25 mmol) was slowly added. The reaction mixture was cooled to 0–5 °C and 5 M

**Scheme 1** Schematic diagram of selective turn-on fluorescence sensor fabrication for  $\text{Zn}^{2+}$ ,  $\text{Cu}^{2+}$  and  $\text{Fe}^{3+}$



$\text{NaNO}_2$  ( $0.27 \text{ mL mmol}^{-1}$  of substrate) was added drop wise; the mixture was stirred for 30 min. The excess  $\text{HNO}_2$  ( $\text{I}_2$ -starch test) was destroyed using amidosulfuric acid.

#### Azo Coupling

To a solution of 2-aminonaphthalene (7 mmol) in  $\text{H}_2\text{O}$  (10.0 mL), concentrated  $\text{HCl}$  (1.0 mL; 9 mmol) was added and the mixture heated for 10 min. After cooling, in an ice-acetone bath, the diazonium salt solution was added drop wise, pH was adjusted to 5 using a 5 M  $\text{NaOH}$  solution, and the mixture stirred for 1 h. When the coupling was complete (H-acid test), pH was adjusted to 7, the precipitated dye was filtered off and used in the next step without drying.

#### Oxidation With Copper Acetate

To the above dye, pyridine (5.0 mL),  $\text{H}_2\text{O}$  (2.0 mL) and  $\text{Cu}(\text{OAc})_2$  (2.5 g; 13.8 mmol) were added, the mixture was refluxed for 15 min and poured into water. The precipitated solid was filtered off and dried. Recrystallization from hot ethanol afforded the final compound.

Yield: 1.2 g, 49 %.

$^1\text{H}$  NMR (300 MHz,  $\text{DMSO-d}_6$ ): 7.71–7.80 (m, 2H (H-7, H-8), 7.91 (d,  $J=9.3$  Hz, 1H, H-4), 7.94 (d,  $J=9.0$  Hz, 1H, H-5), 8.08 (dd,  $J=2.1, 6.6$  Hz, 1H, H-9), 8.16 (d,  $J=9.0$  Hz, 2H, H-2', H-6'), 8.54 (d,  $J=9.0$  Hz, 2H, H-3', H-5'), 8.55 (dd,  $J=2.1, 6.6$  Hz, 1H, H-6).

$^{13}\text{C}$  NMR (75.4 MHz,  $\text{DMSO-d}_6$ ): 116.20 (C-4), 120.04 (C-3', C-5'), 122.93 (C-6), 123.75 (C-9a), 128.27 and

128.50 (C-7, C-8), 129.40 (C-9), 129.91 (C-2', C-6'), 130.94 (C-5), 132.23 (C-3a), 139.57 (C-4'), 142.67 (C-1'), 142.83 (C-9b), 143.66 (C-3a), 160.22 (C=O)

HRMS calcd for  $\text{C}_{17}\text{H}_{11}\text{N}_3\text{O}_2$ : 289.0851. Found: (M-1)+288.0849.

#### General Procedure for the Synthesis of Ligand Functionalized AgNPs

Silver nitrate (5 ml of  $10^{-3}$  M) was added into VP and ILP (5 ml,  $10^{-3}$  M) solution under stirring at room temperature. The immediate appearance of yellow colour indicated the reduction of silver ion into AgNPs. The solution was allowed to stir at room temperature for another 10 min. The reactions were repeated at least three times to confirm the reproducibility of NPs formation. The characterization of the synthesized AgNPs was carried out after allowing the solution to stand at room temperature for more than 1 week. This was preserved as a stock solution for metal nanoparticles fluorescence quenching experiments.

#### Characterization

A Bruker DRX500 spectrometer recorded  $^1\text{H}$  and  $^{13}\text{C}$  NMR spectra of the compound at 400 MHz and 100 MHz respectively.  $^1\text{H}$  chemical shifts were reported in ppm downfield from tetramethylsilane (TMS,  $\delta$  scale with the solvent resonances as internal standards). Absorption and fluorescence spectra were recorded using Perking Elmer Lambda 1050 and Jasco fluorescence spectrometer-FP-8200 instruments.

Fluorescence metal ion selectivity measurement was performed by adding excess concentration of metal salt (10:1)

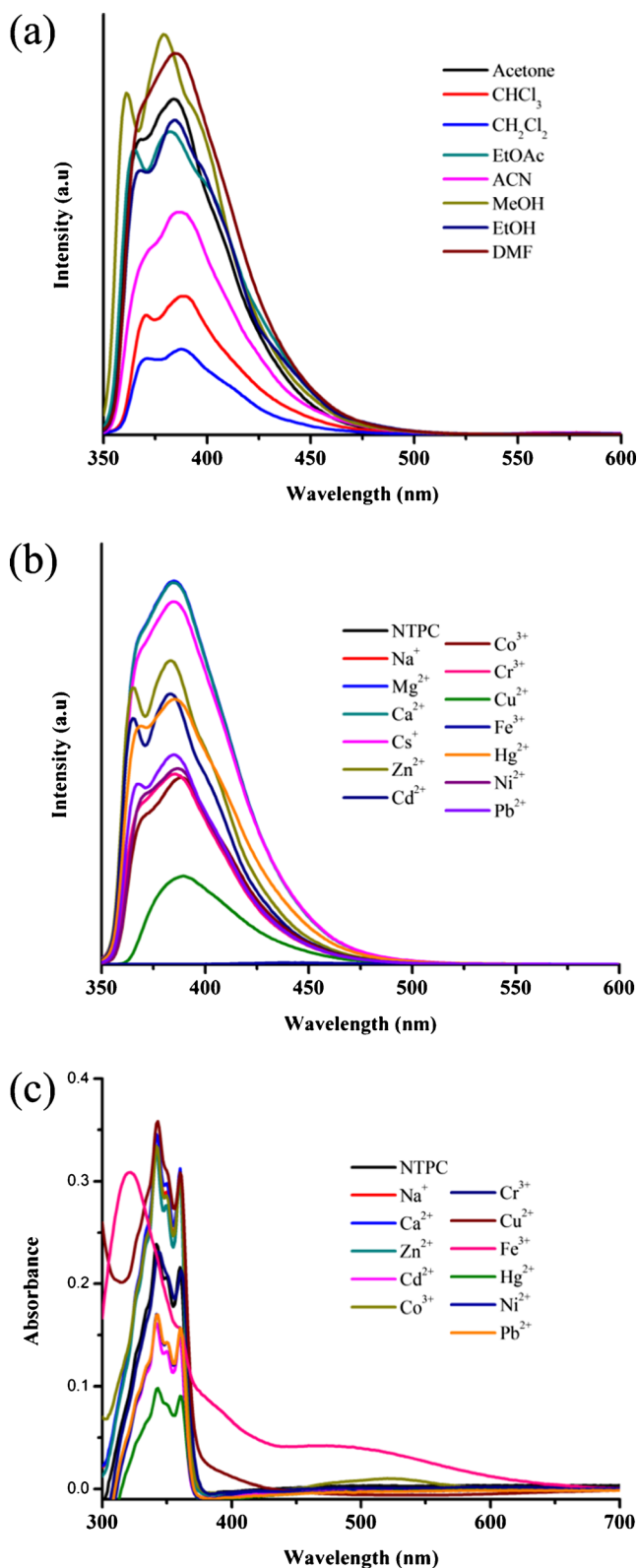


**Fig. 1** (a) NTPC fluorescence in different solvents. NTPC (b) fluorescence and (c) absorption with different metal ions in DMF

into NTPC solution. FT-IR spectroscopy measurements were carried out on a Perkin–Elmer Spectrum-One instrument in the diffuse reflectance mode at a resolution of 4 cm<sup>-1</sup> in KBr pellets.

The size and morphology of AgNPs were investigated using HR-TEM (High Resolution Transmission Electron Microscopy). Samples for TEM measurements were prepared by placing a drop of NPs solution on the graphite grid and drying it in vacuum. Transmission electron micrographs were taken using JEOL JEM-2100 F operated at an accelerated voltage of 200 kV and an ultra high-resolution pole piece.

## Results and Discussion

Pure NTPC dissolves only in organic solvents and shows weak to strong fluorescence with almost same  $\lambda_{\text{max}}$  from different

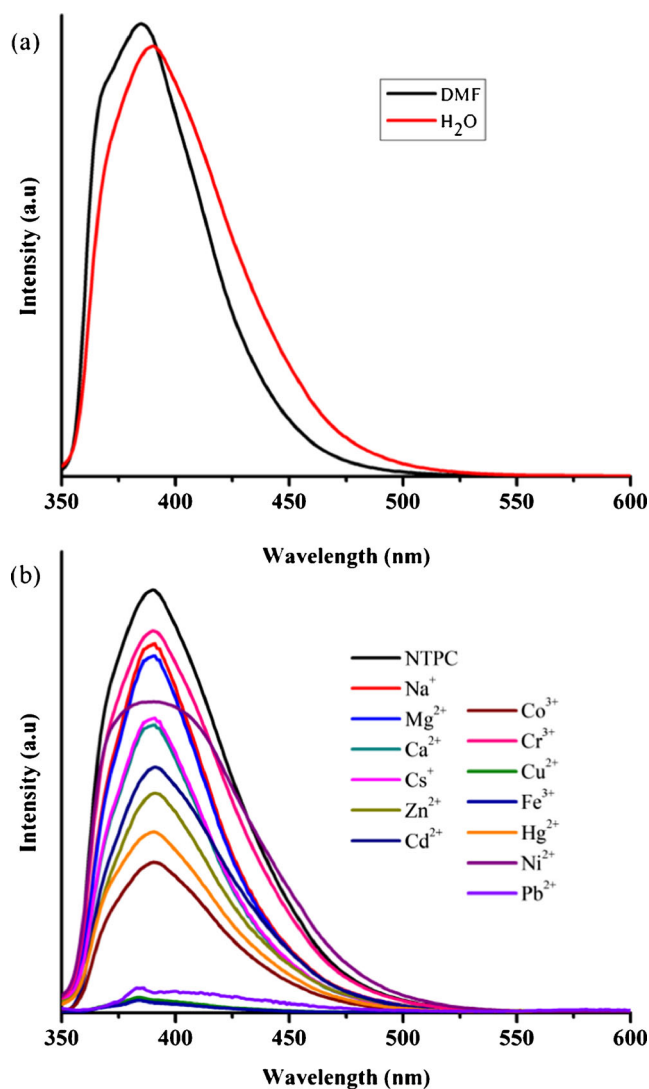


**Fig. 2** Fluorescence of NTPC in (a) DMF and water and (b) with different metal ions in water



solvents (Fig. 1a). In chloroform and dichloromethane, NTPC showed weak fluorescence at  $\lambda_{\text{max}}=384$  nm (quantum yield,  $\Phi_F=0.25$  on comparison with quinine sulfate), but in DMF it showed strong fluorescence ( $\Phi_F=0.71$ ). Acetone, methanol and ethanol solution showed similar fluorescence intensity. It was found that the position and shape of the fluorescence spectrum is independent of the excitation wavelength both at 342 or 360 nm. The small Stokes shift of the NTPC, demonstrated that, there is no substantial geometry difference between vertical and relaxed (fluorescence) states, which could be related to the planarity of the triazole chromophore. The metal ion sensor studies of NTPC in DMF exhibited complete fluorescence quenching for  $\text{Fe}^{3+}$  but only at very high concentration ( $500 \mu\text{l}$  of  $10^{-2}$  M, Fig. 1b). Absorption spectra of NTPC in DMF showed two absorption peaks at 342 and 360 nm (Fig. 1c) and these band corresponds to  $\pi$ - $\pi^*$  transition. Addition of different metal ions did not show significant change in the NTPC absorption except with  $\text{Cu}^{2+}$  and  $\text{Fe}^{3+}$ . Addition of  $\text{Cu}^{2+}$  with NTPC showed slightly red shifted  $\lambda_{\text{cut-off}}$  without changing absorption peak position. However, NTPC with  $\text{Fe}^{3+}$  exhibited completely different absorption spectrum and confirms the selective interaction of NTPC with  $\text{Fe}^{3+}$ . Although pure NTPC is not soluble in water, conversion of NTPC carboxylic acid into sodium salt makes it soluble and importantly it retained its strong fluorescence in water also (Fig. 2a). The small hump appeared at 368 nm in DMF has

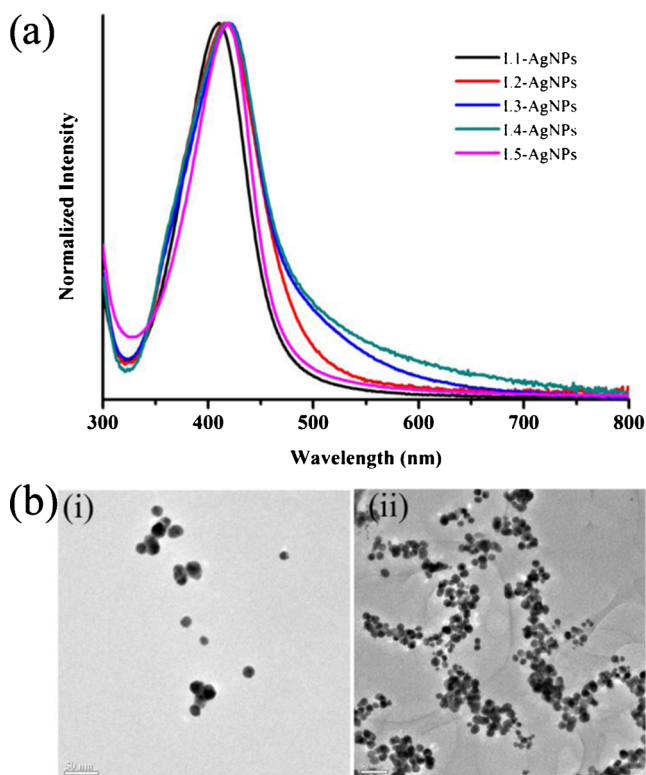


**Fig. 3** Absorption spectra of (a) L-AgNPs and (b) HR-TEM of (i) L3-AgNPs and (ii) L5-AgNPs

disappeared and showed small red shift in the  $\lambda_{\text{max}}$  (384 to 391 nm). Metal ion sensor studies in water also showed selective quenching of NTPC fluorescence with three metal cations,  $\text{Fe}^{3+}$ ,  $\text{Cu}^{2+}$  and  $\text{Pb}^{2+}$  (Fig. 2b) but again only at higher concentration ( $500 \mu\text{l}$  of  $10^{-2}$  M). These results suggest that  $\text{Pb}^{2+}$ ,  $\text{Cu}^{2+}$  and  $\text{Fe}^{3+}$  might be forming coordination complexes with NTPC at higher concentration. The mechanism of NTPC fluorescence quenching might be due to the electronic energy transfer (EET) and/or photo-induced electron transfer (PET) from ligand to metal centre that has paramagnetic unfilled electronic configuration of  $d$ -orbital [49].

AgNPs functionalized with amino acid attached phenolic chelating ligand was yellow and transparent, indicating the good dispersity in water. Phenolic ligands with different amino acids were used in the synthesis of AgNPs (Scheme 1). The absorption spectrum of L-AgNPs showed a typical and intense absorption peak between 409 nm to 418 nm which is due to surface plasmon resonance vibration (Fig. 3a) [50]. The

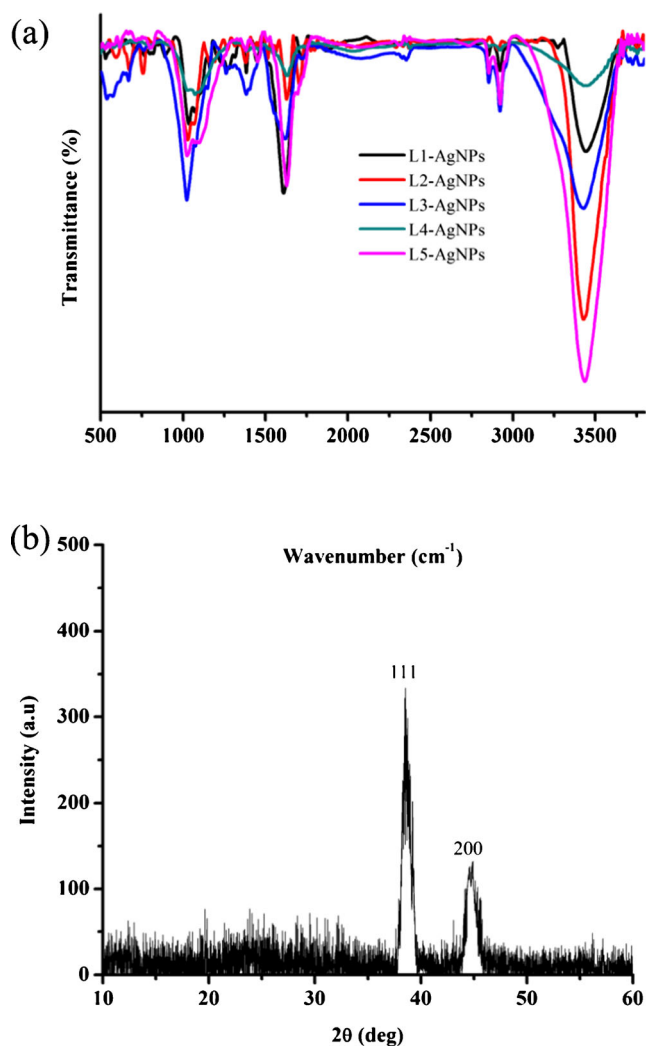


**Fig. 4** (a) IR spectra of L-AgNPs and (b) PXRD patterns of L3-AgNPs

synthesized AgNPs size and morphology were characterized by using HR-TEM that confirmed the formation of poly-dispersed spherical crystalline AgNPs (Fig. 3b). The amino acid attached phenolic chelating ligand is expected to provide metal ions interacting surface functionality to the AgNPs. Prominent IR bands observed at 3,434, 2,931, 2,853, 1,696, 1,615, 1,430 and 1,385  $\text{cm}^{-1}$  for all samples confirmed the surface functionalization of AgNPs by amino acid attached phenolic ligands (Fig. 4a). The phase structure of the prepared AgNPs was characterized by powder X-ray diffraction (XRD). Figure 4b shows the representative case for AgNPs prepared by using L3 and peak at 38.2 and 44.1 agree well with the (111) and (200) diffraction of face centered cubic (fcc) silver (JCPDS file no. 04–0783). The other two peaks assigned to the glass matrix.

Assembling fluorophore near the vicinity of metallic nanoparticles surface is known to quench the fluorescence strongly

[28–31]. The hydrogen bonding functionality of both NTPC and amino acid based phenolic ligands are expected to facilitate closer assembling of fluorophore near NPs surface.

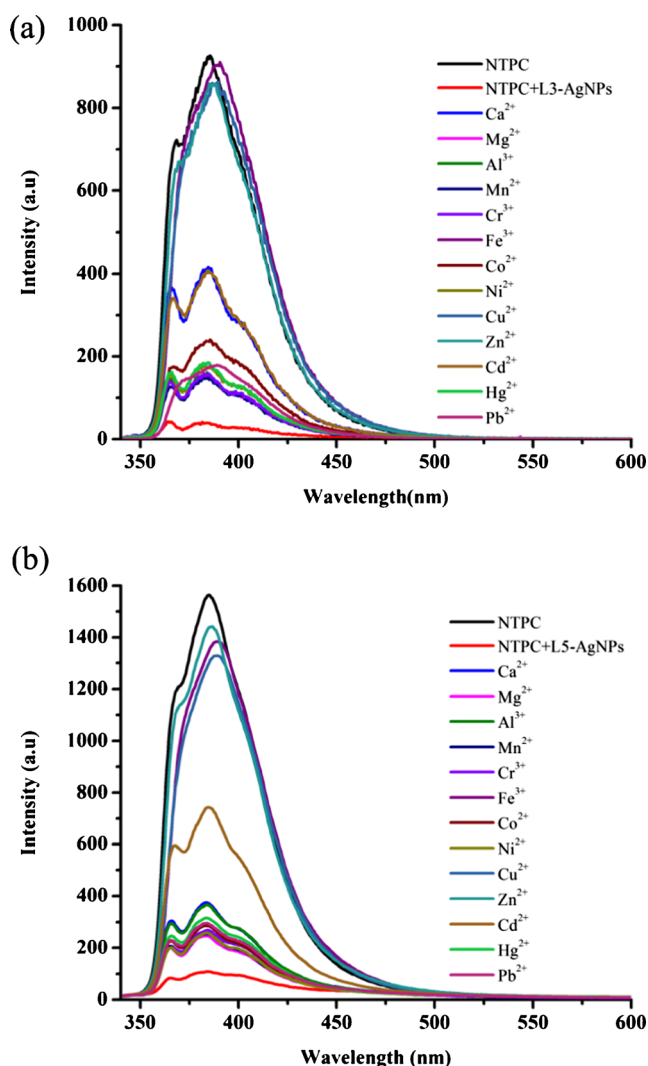


**Fig. 5** Turn-on fluorescence studies of (a) NTPC-L3-AgNPs and (b) NTPC-L5-AgNPs with different metal ions ( $\lambda_{\text{exc}}=340$  nm)

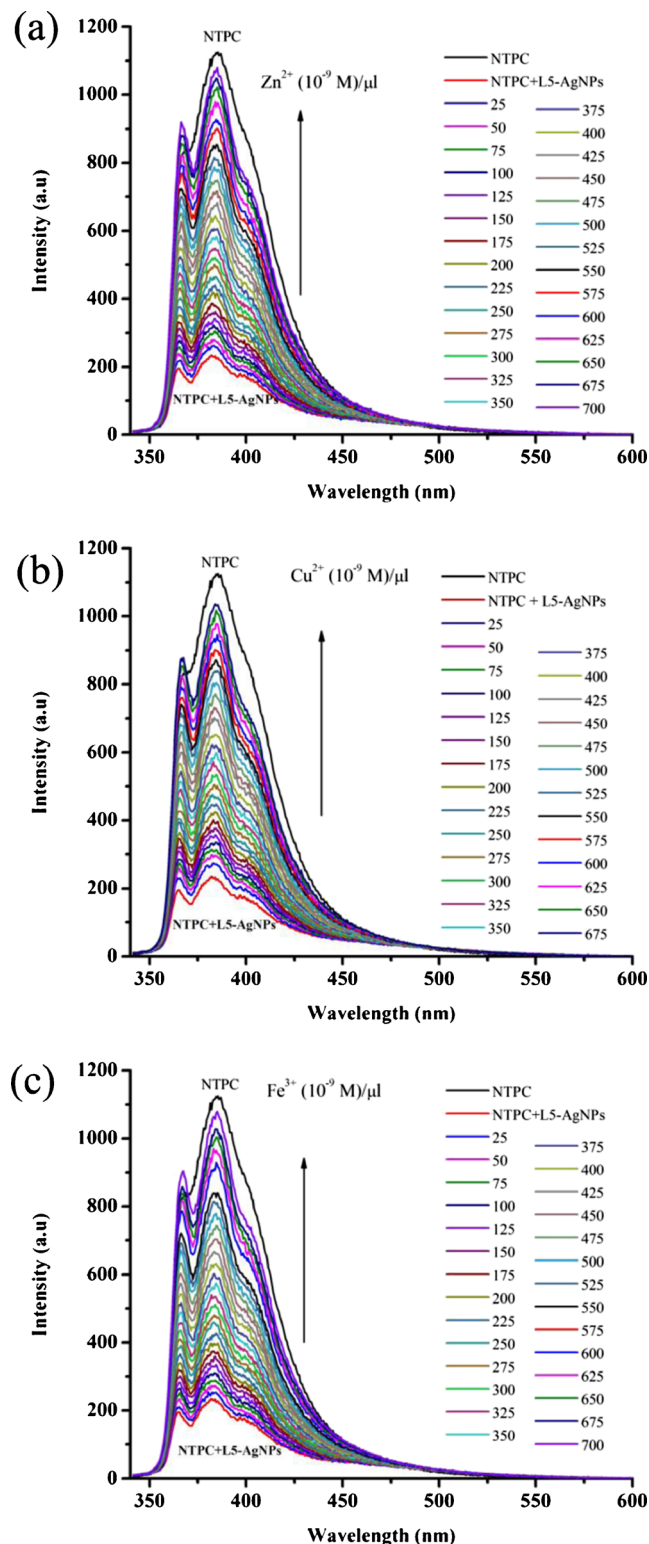


**Fig. 6** Concentration dependent studies of turn-on fluorescence with (a)  $\text{Zn}^{2+}$ , (b)  $\text{Cu}^{2+}$  and (c)  $\text{Fe}^{3+}$  in water ( $\lambda_{\text{exc}}=340$  nm)

Addition of L-AgNPs (100  $\mu\text{l}$  of  $10^{-4}$  M) into aqueous solution of NTPC (200  $\mu\text{l}$  of  $10^{-6}$  M of DMF solution in 2 ml of water) completely quenched the fluorescence (Fig. 5, S). Amino acid attached phenolic chelating ligands, L, are strongly coordinating ligands for metal ions and several coordination polymers with intriguing solid state structures have been generated by self-assembling L with metal ions [45–47]. Hence coordination complex formation of metal ions with L-AgNPs is expected to separate NTPC fluorophore from the AgNPs vicinity. The separation would lead to the regeneration of NTPC fluorescence. Different metal ions ( $\text{Na}^+$ ,  $\text{Mg}^{2+}$ ,  $\text{Cs}^{2+}$ ,  $\text{Ca}^{2+}$ ,  $\text{Zn}^{2+}$ ,  $\text{Cd}^{2+}$ ,  $\text{Cr}^{3+}$ ,  $\text{Hg}^{2+}$ ,  $\text{Cu}^{2+}$ ,  $\text{Fe}^{3+}$ ,  $\text{Pb}^{2+}$  and  $\text{Ni}^{2+}$ ) were added into NTPC-L-AgNPs and monitored the fluorescence change. Interestingly, all NTPC-L-AgNPs samples showed selective turn-on fluorescence for biologically important  $\text{Zn}^{2+}$ ,  $\text{Cu}^{2+}$  and  $\text{Fe}^{3+}$  metal ions in aqueous solution. Figure 5 shows the turn-on fluorescence of NTPC-L3-AgNPs and NTPC-L5-AgNPs selectively with  $\text{Zn}^{2+}$ ,  $\text{Cu}^{2+}$  and  $\text{Fe}^{3+}$  in aqueous solution. Addition of other metal ions either showed partial regeneration of fluorescence or no fluorescence regeneration. The observed fluorescence turn-on for  $\text{Zn}^{2+}$ ,  $\text{Cu}^{2+}$  and  $\text{Fe}^{3+}$  metal ions was due to the formation of metal coordination complex with L-AgNPs that separates NTPC fluorophore from the AgNPs surface vicinity. Concentration dependent studies of NTPC-L5-AgNPs showed complete regeneration of fluorescence intensity by addition of 650–700  $\mu\text{l}$  of  $\text{Zn}^{2+}$ ,  $\text{Cu}^{2+}$  and  $\text{Fe}^{3+}$  metal ions at ppb level (Fig. 6). Absorption

studies were performed to get the insight of the complex formation with L-AgNPs (Fig. 7a). NTPC-L5-AgNPs showed both absorption corresponding to NTPC and L5-AgNPs. However, absorption peak of L5-AgNPs almost vanished with  $\text{Zn}^{2+}$ ,  $\text{Cu}^{2+}$  and  $\text{Fe}^{3+}$  metal ions that confirm the formation of coordination complex with L5. The metal coordination with L is expected to produce smaller aggregates of AgNPs. HR-EM analysis of  $\text{Fe}^{3+}$  metal ions added NTPC-L3- and L5-AgNPs complexes clearly show the aggregate formation and supports the metal coordination (Fig. 7b).

Interestingly,  $\text{Mn}^{2+}$  addition into NTPC-L-AgNPs did not show any change of NTPC fluorescence or regeneration immediately. However, after 12 h, all samples with  $\text{Mn}^{2+}$  exhibited strongly red shifted fluorescence at 500 nm (Fig. 8a). Other metal ions did not show any such fluorescence shift. Fluorescence spectra of all  $\text{Mn}^{2+}$  added samples showed two  $\lambda_{\text{max}}$ ; one at 500 nm and other at 385 nm.  $\text{Mn}^{2+}$  with NTPC-L3 and L5-AgNPs exhibited strong intensity at 500 nm along

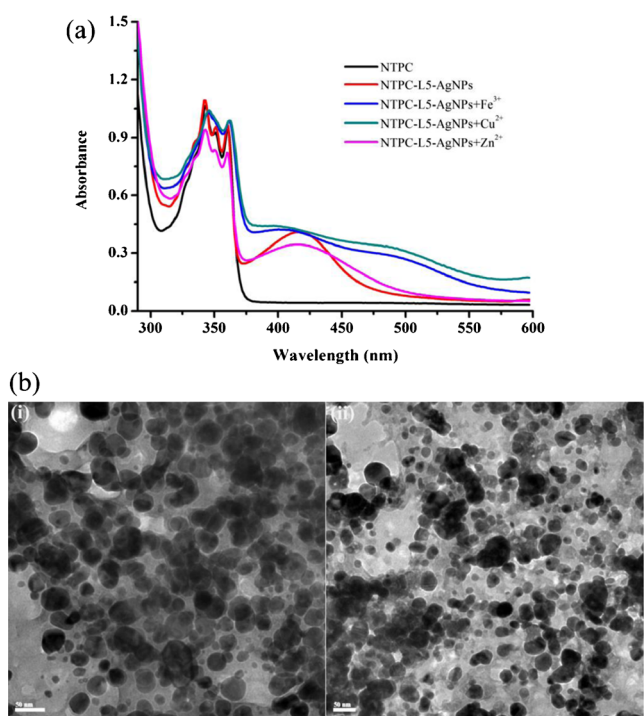


**Fig. 7** (a) Absorption spectra of NTPC-L5-AgNPs with  $\text{Zn}^{2+}$ ,  $\text{Cu}^{2+}$  and  $\text{Fe}^{3+}$  in water and (b) HR-TEM images of (i) NTPC-L3-AgNPs and (ii) NTPC-L5-AgNPs with  $\text{Fe}^{3+}$

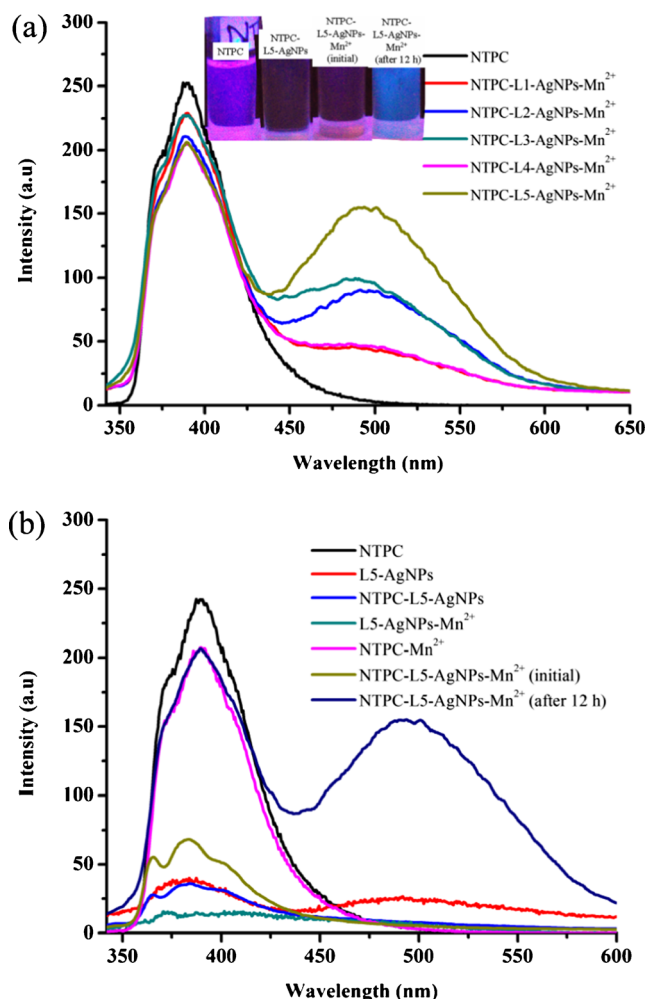


**Fig. 8** (a) Fluorescence spectra of  $\text{Mn}^{2+}$  with NTPC-L-AgNPs and (b) controlled experiment. Digital images of fluorescence changes are shown in the inset



with the 385 nm fluorescence. All other samples showed weak fluorescence at 500 nm and strong fluorescence at 385 nm. Controlled experiments were performed with different combination of  $Mn^{2+}$  to get insight for the fluorescence change (Fig. 8b).  $Mn^{2+}$ -L4-AgNPs (without NTPC),  $Mn^{2+}$ -NTPC-L4 (without AgNPs) and  $Mn^{2+}$ -NTPC (without L4-AgNPs) did not show any fluorescence change even after 24 h. These studies indicate that presence of AgNPs, L as well as NTPC fluorophore is important for the fluorescence red shift. Absorption studies of  $Mn^{2+}$  with NTPC-L5-AgNPs revealed no change immediately. However, absorption of L5-AgNPs was completely disappeared after 12 h with appearance of new peak at 500 nm. (Fig. 9a). HR-TEM studies confirmed the presence of AgNPs in  $Mn^{2+}$  added NTPC-L5-AgNPs but with aggregated form (Fig. 9b). This might be due to the formation coordination complex very slowly.

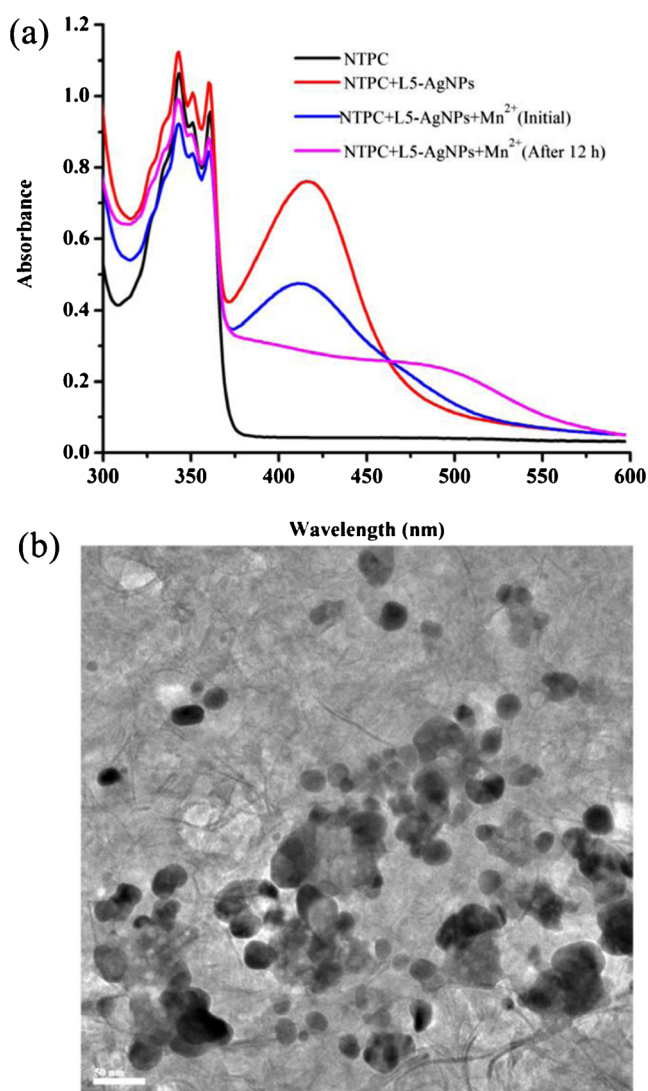


**Fig. 9** (a) Absorption and (b) HR-TEM image of  $Mn^{2+}$  with NTPC-L5-AgNPs

## Conclusion

We have demonstrated a simple approach in developing turn-on fluorescent sensor based on AgNPs and organic fluorophore hybrid materials for heavy metal ions including paramagnetic metal ions by exploiting unique characteristics of noble metal nanoparticles on the organic fluorophore fluorescence. Assembling organic fluorophore, NTPC, near the vicinity of AgNPs surface via hydrogen bonding interactions of capping ligands with NTPC strongly quenches the organic fluorescence. The strong and selective coordination of amino acid attached phenolic chelating ligands with biologically important metal ions,  $Zn^{2+}$ ,  $Cu^{2+}$  and  $Fe^{3+}$ , separates fluorophore from AgNPs surface and turn-on the NTPC fluorescence. Concentration dependent studies showed selective detection of  $Zn^{2+}$ ,  $Cu^{2+}$  and  $Fe^{3+}$  metal ions in aqueous solution up to ppb level. Absorption and HR-TEM studies further support the formation of coordination complexes with metal ions. Change of amino acids did not show any influence on the metal ion selectivity.  $Mn^{2+}$  selectively red shifted the NTPC fluorescence  $\lambda_{max}$  with all samples after 12 h. It is expected that fine tuning of metal ion interacting capping ligands of NPs would lead to highly selective and sensitive turn-on fluorescence sensor for paramagnetic heavy metal ions in aqueous solution.

**Acknowledgments** Financial supports from Department of Science and Technology, New Delhi, India (DST Fast Track Scheme No. SR/FT/CS-03/2011 (G), SR/FT/CS-10/2011 and SR/FST/ETI-284/2011(c)) are acknowledged with gratitude.

## References

- Valeur B, Leray I (2000) *Coord Chem Rev* 205:3–40
- Pawley JB (1995) *Handbook of biological confocal microscopy*. Plenum, New York
- Lichtman JW, Conchello J-A (2005) *Nat Methods* 2:910–919
- De Silva AP, Gunaratne HQN, Gunlaugsson TA, Huxley JM, McCoy CP, Rademacher JT, Rice TE (1997) *Chem Rev* 97:1515–1566
- Ueno T, Nagano TO (2011) *Nat Methods* 8:642–645
- Gaggelli E, Kozlowski H, Valensin D, Valensin G (2006) *Chem Rev* 106:1995–2044
- Berg JM, Shi Y (1996) *Science* 271:1081–1085
- Bush AI (2000) *Curr Opin Chem Biol* 4:184–191
- Meneghini R (1997) *Free Radical Biol Med* 23:783–792
- Andrews NCN (1999) *Engl J Med* 341:1986–1995
- Touati D (2000) *Arch Biochem Biophys* 373:1–6
- Kim JS, Quang DT (2007) *Chem Rev* 107:3780–3799
- Aragay G, Pons J, Merkoci A (2011) *Chem Rev* 111:3433–3458
- Chen X, Nam S-W, Jou MJ, Kim Y, Kim S-J, Park S, Yoon J (2008) *Org Lett* 10:5235–5238
- Nolan EM, Jaworski J, Okamoto K-I, Hayashi Y, Sheng M, Lippard SJ (2005) *J Am Chem Soc* 127:16812–16823
- Jung HS, Kwon PS, Lee JW, Kim J, Hong CS, Kim JW, Yan S, Lee JY, Lee JH, Joo T, Kim JS (2009) *J Am Chem Soc* 131:2008–2012
- Anthony SP (2012) *Chem Asian J* 7:374–379



18. Royzen M, Dai Z, Canary JW (2005) *J Am Chem Soc* 127:1612–1613
19. Hu ZQ, Lin CS, Wang XM, Ding L, Cui CL, Liu SF, Lu HY (2010) *Chem Commun* 46:3765–3767
20. Malinsky MD, Kelly KL, Schatz GC, Van Duyne RP (2001) *J Am Chem Soc* 123:1471–1482
21. Zhang XB, Kong RM, Lu Y (2011) *Ann Rev Anal Chem* 4:105–128
22. Xu X, Daniel WL, Wei W, Mirkin CA (2010) *Small* 6:623–626
23. Han CP, Zhang L, Li HB (2009) *Chem Commun* 3545–3547
24. Li HB, Cui ZM, Han CP (2009) *Sens Actuators B: Chem* 143:87–92
25. Roy B, Bairi P, Nandi AK (2011) *Analyst* 136:3605–3607
26. Ravi SS, Christena LR, SaiSubramanian N, Anthony SP (2013) *Analyst* 138:4370–4377
27. Karthiga D, Anthony SP (2013) *RSC Adv* 3:16765–16774
28. Avouris P, Persson BNJ (1984) *J Phys Chem* 88:837–848
29. Cnossen G, Drabe KE, Wiersma DA (1993) *J Chem Phys* 98:5276–5280
30. Lakowicz JR (2001) *Anal Biochem* 298:1–24
31. Aslan K, Víctor H, Luna P (2004) *J Flu* 4:401–405
32. Sokolov K, Chumanov G, Cotton TM (1998) *Anal Chem* 70:3898–3905
33. Liebermann T, Knoll W (2000) *Colloids Surf A* 171:115–130
34. Gryczynski I, Malicka J, Shen Y, Gryczynski Z, Lakowicz JR (2002) *J Phys Chem B* 106:2191–2195
35. Anker JN, Hall WP, Lyandres O, Shah NC, Zhao J, Van Duyne RP (2008) *Nat Mater* 7:442–453
36. Bardhan R, Grady NK, Cole JR, Joshi A, Halas NJ (2009) *ACS Nano* 3:744–752
37. Chan YH, Chen JX, Wark SE, Skiles SL, Son DH, Batteas JD (2009) *ACS Nano* 3:1735–1744
38. Phadke RC, Rangnekar DW (1986) *J Chem Tech Biotech* 36:230–235
39. Rangnekar DW, Tagdiwala PV (1986) *Dyes Pigments* 7:289–298
40. Esteves AP, Rodrigues LM, Silva ME, Oliveira-Campos AMF, Machalicky O, Mendonça A (2005) *Tetrahedron* 61:25–32
41. Birks JB (1977) *Fluorescence quantum yield measurements*. National Bureau of Standards, Washington, Special Publication No. 466
42. Lund RB, Bass LW, (1984) *Ciba-Geigy A.-G., Switz., Ger. Offen. DE3334490*.
43. Dobás J, PirkI J (1960) *Coll Czechoslovak Chem Commun* 25:912–918
44. Jacob JA, Mahal HS, Biswas N, Mukherjee T, Kapoor S (2008) *Langmuir* 24:528–533
45. Ranford JD, Vittal JJ, Wu D (1998) *Angew Chem Int Ed* 37:114–1116
46. Ranford JD, Vittal JJ, Wu D, Yang X (1999) *Angew Chem Int Ed* 38: 3498–3501
47. Yang X, Ranford JD, Vittal JJ (2004) *Cryst Growth Des* 4: 781–788
48. Oliveira-Campos AMF, Rodrigues LM, Esteves AP, Silva ME, Sivasubramanian A, Hrdina R, Soares GMB, Pinto TAD, Machalicky O (2010) *Dye and Pigments* 87:188–193
49. Ma L, Luo W, Quinn PJ, Liu Z, Hider RC (2004) *Design. J Med Chem* 47:6349–6362
50. Mulvaney P (1996) *Langmuir* 12:788–800